JOURNAL OF SOLID STATE CHEMISTRY **132,** 372–381 (1997)
ARTICLE NO. SC977476

The Cr-Substituted Spinel Mn Oxides $LiCr_yMn_{2-y}O_4$ ($0 \leq y \leq 1$): Rietveld Analysis of the Structure Modifications Induced by the Electrochemical Lithium Deintercalation

C. Sigala, A. Verbaere,[1] J. L. Mansot, D. Guyomard, Y. Piffard, and M. Tournoux

Laboratoire de Chimie des Solides, IMN, 2, rue de la Houssinière, B.P. 32229, 44322 Nantes Cedex 03, France

Received December 5, 1996; in revised form May 8, 1997; accepted May 21, 1997

The electrochemical study of $LiCr_y^{III}Mn_{1-y}^{III}Mn^{IV}O_4$ compounds, $0 \leq y \leq 1$, between 3.5 and 5.4 V vs Li metal, shows that the Cr substitution is beneficial to the overall performances (capacity, specific energy, and cyclability) for $y \leq 0.62$, and that $y = 0.25$ gives the best results. For $y > 0.62$, the cyclability is worse than for $LiMn_2O_4$, and for $y \geq 0.75$ the capacity fading becomes very fast. The electron energy loss spectroscopy study confirms that the deintercalation in the range 3.5–4.3 V corresponds to a Mn^{III}–Mn^{IV} oxidation. Further deintercalation between 4.3 and 5.1 V mainly corresponds to a Cr^{III}–Cr^{IV} oxidation with, however, the formation of a significant amount of Cr^{VI} for the highest Cr content $y = 0.75$. In the starting compounds LiM_2O_4, M = Cr, Mn, Rietveld refinements show that the 8*a* and 16*d* sites of the spinel structure are occupied by Li and M, respectively. The Li deintercalation up to 5.1 V induces structural defects which do not disappear completely upon the subsequent intercalation down to 3.5 V; their concentration increases upon cycling. Such defects consist of M cations occupying an 8*a* site ("Td defect") or a 16*c* site ("16*c* defect"), instead of 16*d*. Both defects imply a lowering of the tetrahedral Li concentration which accounts for the experimental capacity loss upon cycling.

INTRODUCTION

The electrochemical properties of members of the spinel solid solution $LiCr_yMn_{2-y}O_4$ ($0 \leq y \leq 1$), as positive electrode materials for Li batteries were previously described (1, 2). It was shown that upon substitution of Mn^{III} by Cr^{III} a capacity decrease occurs in the voltage range 3.5–4.3 V (all voltages reported in this article are given versus Li metal). More recently, an electrochemical study of the title compounds extended up to 5.4 V showed that the capacity lost upon this substitution could be recovered at higher voltage (3). However, the strong dependence of the electrochemical properties on the Cr content led us to undertake Rietveld refinements on materials corresponding to various y values, at different steps of the deintercalation–intercalation reaction, and after several charge/discharge cycles (the title compounds remain crystalline even after 300 cycles which enables such a structural study).

This paper presents a Rietveld analysis of the structure modifications that are induced by the electrochemical treatment of the title compounds along with an investigation of the oxidation states of Cr and Mn cations by electron energy loss spectoscopy (EELS).

EXPERIMENTAL

The starting compounds $LiCr_yMn_{2-y}O_4$, $0 \leq y \leq 1$, were prepared by solid state reaction at 750°C as previously indicated (3). Chemical analyses of Li and Mn were made by flame absorption spectrometry. They agree with the above mentioned formulas. The Cr : Mn ratios as well as the sample homogeneity were verified using a microprobe and energy dispersive X-ray spectrometry in a Jeol JSM35 electron microscope. The crystals are cuboctahedra, approximately 1 μm in dimension (in agreement with the measured surface areas, all close to $2\ m^2\ g^{-1}$).

$Li_xCr_yMn_{2-y}O_4$ compounds with $x < 1$ were electrochemically prepared (potentiostatic mode) at the end of the major electrochemical reactions, from the starting materials, by charge/discharge of Li batteries (for details, see (3); one charge or discharge within 50 h). The final voltage (3.5, 4.3, or 5.1 V) was maintained until a constant, negligible current was reached. Samples of 10 mg, approximately, were obtained (under inert gas) from each composite positive electrode.

The X-ray powder diffraction (XRPD) patterns were recorded with a Siemens D5000 diffractometer using Cu$K\alpha$ radiation, in the 2θ range 5–120°, with steps of 0.03°(2θ) and a step time of 12 s. As some electrochemically prepared materials were rapidly altered when exposed to air, all $Li_xCr_yMn_{2-y}O_4$ ($x < 1$) samples were protected with a

[1] To whom correspondence should be addressed.

0022-4596/97 $25.00

Kapton film. For each $LiCr_yMn_{2-y}O_4$ starting compound, two data sets, with and without the protective film, were recorded and used in refinements for comparison. Most of the diffraction lines exhibit large intensities; therefore, problems arising in some difference profiles were easily detected. However, as large intensities also lead to underestimated values of the standard deviations σ (4), some refinements from XRPD data obtained with a step time of 2 s were also performed; they indicate that the σ values reported in Table 2 should be multiplied by 1.5, approximately. Accordingly, the errors mentioned in Figs. 6 to 10 correspond to 1.5σ.

For $Li_xCr_yMn_{2-y}O_4$ ($x < 1$) samples, most of the XRPD data were recorded within 2 days after the end of the electrochemical preparation. However, some samples were allowed to relax for 3 months, under inert gas, before the data collection.

The structure refinements were carried out using program GSAS (5). Nearly 20 background points were fixed, and 4 coefficients of a cosine Fourier series were refined, together with the zero point, the cell parameter, and 6 line-profile parameters (second profile function of GSAS). As the protective film strongly lowered the intensity of the first line at low 2θ angle, the 2θ range used in the refinements was limited to 34–120°. In this range, the lowering was weak and looked like an absorption effect leading to slightly negative thermal parameters U. An absorption coefficient was adjusted in order to obtain plausible U values together with a satisfactory fit. Comparative refinements of the starting compounds have shown that the collection and refinement conditions did not influence the structural results significantly.

The electron energy loss spectroscopy study was performed using a Philips CM30 microscope equipped with a Gatan 666 parallel spectrometer. For an easier analysis, the $Li_xCr_yMn_{2-y}O_4$ ($x < 1$) samples were prepared without organic binder; the sample preparation (grid) and the transfer into the microscope were performed under inert gas. In order to avoid the influence of the electron beam on the spectra, the samples were cooled down to 120 K, and the irradiation time was reduced to 0.1 s. For each sample, spectra were accumulated until any spectrum shift was observed. The lines at the L_3 and L_2 edges of Cr and Mn were compared with those in MnO, Mn_2O_3, MnO_2, Cr_2O_3, CrO_2, and CrO_3. The oxidation states of Cr and Mn were inferred from both the L_3 line positions and the L_2/L_3 line intensity ratios, according to a method described in (*6*). The error in oxidation states is approximately 0.1.

RESULTS

Summary of the Electrochemical Studies

Typical discharge curves obtained after a charge up to 5.4 V are presented in Fig. 1. They show that the reversible

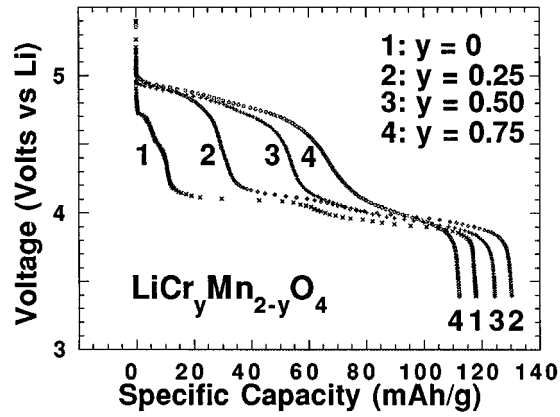

FIG. 1. First discharge curves down to 3.4 V at C/15 of $Li_xCr_yMn_{2-y}O_4$, after an initial charge at C/6 up to 5.4 V.

Li intercalation occurs in two steps at about 4.9 and 4 V. In agreement with the previous studies (1, 2), the capacity of the 4-V process decreases with increasing chromium content. On the other hand, the capacity of the 4.9 V process increases with y. The chromium substitution is beneficial to the overall capacity for $y \leq 0.62$ and to the specific energy as well, due to a higher average intercalation voltage than in the case of $LiMn_2O_4$ (3). For $y > 0.62$ the capacity decreases with y and the average voltage remains constant. Furthermore, a lower capacity loss upon cycling is observed for $y \leq 0.5$ compared to the nonsubstituted $LiMn_2O_4$ material, whereas the capacity fading is very fast for $y \geq 0.75$ (Fig. 2). As a summary, a break is observed in the variation of many electrochemical parameters with y, such as capacity, average voltage, and cyclability. At this point, one wonders why so

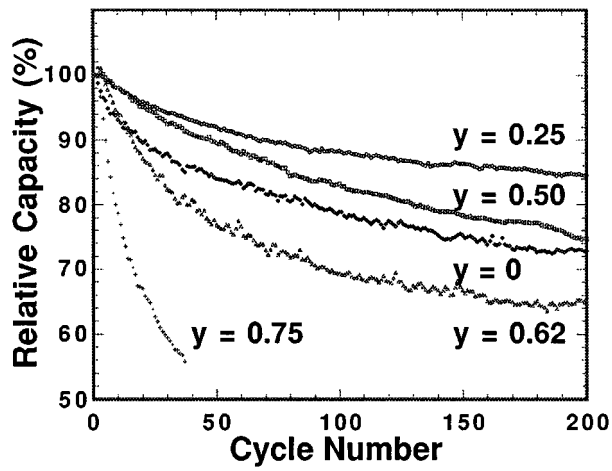

FIG. 2. Relative capacity (in percent of the initial capacity) variation upon cycling of $Li_xCr_yMn_{2-y}O_4$ materials (charges at C/6, discharges at C/15).

different behaviors can arise. The studies which follow were undertaken with the aim to answer this question.

EELS Study

The oxidation states of Cr and Mn were determined in the starting compounds (hereafter named SC($y*10^2$)) and in the $Li_xCr_yMn_{2-y}O_4$ ($x < 1$) compounds with $y = 0.25$ and 0.75 at the following voltages: 4.3 V (first charge, samples hereafter named C4.3(25) and C4.3(75), respectively), 5.1 V (first charge, samples C5.1(25) and C5.1(75)), and 4.3 V (subsequent first discharge, samples D4.3(25) and D4.3(75)). Table 1 shows that, in the SCs, the values obtained for Cr and Mn are in good agreement with the expected formula $Li(Cr_y^{III}Mn_{1-y}^{III})Mn^{IV}O_4$. It also indicates that a reversible Mn^{III} to Mn^{IV} oxidation occurs in the range 3.5–4.3 V, whereas a reversible Cr^{III} to Cr^{IV} oxidation is observed in the higher voltage range 4.3–5.1 V.

However, the shape of some Cr–$L_{2,3}$ and Mn–$L_{2,3}$ lines strongly suggest a less simple situation. For chromium, the two fully oxidized samples C5.1(25) and C5.1(75) lead to slightly different $L_{2,3}$ line profiles as compared to C4.3(25) and C4.3(75), with a larger linewidth likely due to a small amount of Cr^{VI}.

Furthermore, for all the electrochemically prepared samples, the Mn–L_3 line exhibits a shoulder indicating a small amount of Mn^{III}. In the case of C4.3(25) and C4.3(75) this shoulder is very weak in fair agreement with the very low Mn^{III} content remaining (inferred from the Li content determined by electrochemical titration). In $Li_xCr_yMn_{2-y}O_4$ ($x < 1$), a complete oxidation of Mn^{III} would imply a lithium content $x = y$ at 4.3 V, whereas the experimental x values are all slightly larger (3). For C5.1(25), C5.1(75), D4.3(25), and D4.3(75) the shoulders are surprisingly more pronounced and especially in the case of $y = 0.75$ (Fig. 3).

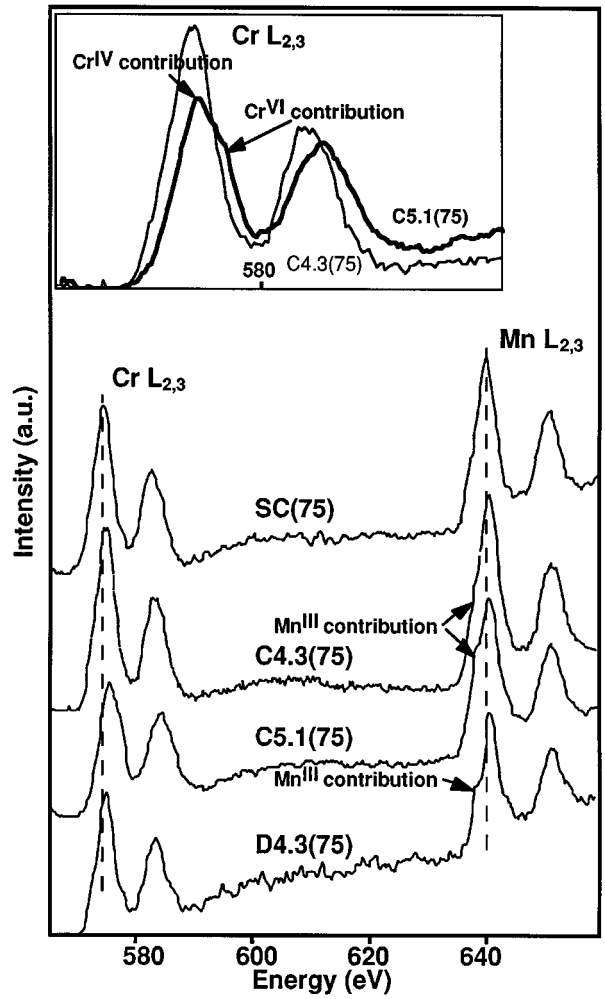

FIG. 3. Evolution of EELS spectra at various steps of the electrochemical treatment (see text) for $y = 0.75$. The inset shows the Cr–$L_{2,3}$ lines on an expanded scale for C4.3 and C5.1 compounds.

TABLE 1
Oxidation States of Cr and Mn Inferred from the EELS Spectra (Expected Values in Parentheses, See Text)

Sample	E_{Mn} (eV)	Mn	E_{Cr} (eV)	Cr
SC(0)	640.0	3.5 (3.50)	—	—
SC(25)	640.3	3.7 (3.57)	575.5	3.0 (3.00)
SC(50)	640.5	3.7 (3.67)	575.4	3.0 (3.00)
SC(75)	640.6	3.9 (3.80)	575.5	3.0 (3.00)
SC(100)	640.9	4.1 (4.00)	575.6	3.1 (3.00)
C4.3(25)	640.8	4.1 (4.00)	575.3	2.9 (3.00)
C5.1(25)	641.0	4.2 (4.00)	576.4	4.0 (4.00)
D4.3(25)	640.6	3.9 (4.00)	575.5	3.0 (3.00)
C4.3(75)	640.8	4.1 (4.00)	575.4	3.0 (3.00)
C5.1(75)	640.8	4.1 (4.00)	576.3	3.9 (4.00)
D4.3(75)	640.7	3.9 (4.00)	575.5	3.0 (3.00)

Note. E is the binding energy at the L_3 line.

EELS results can then be summarized as follows:

(i) at 3.5 V, the initial species are Cr^{III}, Mn^{III}, and Mn^{IV},

(ii) at the end of the first oxidation step (4.3 V), mainly Cr^{III} and Mn^{IV} are observed, which means that Mn^{III} is oxidized first,

(iii) during the second oxidation step up to 5.1 V, Cr^{III} is oxidized to Cr^{IV} mainly; however as the Li content x is not zero some 3+ cations must remain, but, surprisingly these are Mn^{III} mainly. For C5.1(75) the Mn^{III} content is even larger than for C4.3(75). Moreover, there is evidence for Cr in an oxidation state higher than 4, and likely Cr^{VI}.

(iv) Cationic species in D4.3 samples are similar to those observed in C4.3 materials; however there is an indication that some Cr^{VI} formed during the charge up to 5.1 V could remain, and especially for D4.3(75).

Rietveld Refinements

Rietveld refinements were undertaken on SC, C4.3, C5.1, and D4.3 compounds with various Cr contents as well as on materials after n complete charge–discharge cycles between 3.5 and 5.1 V (hereafter named nCY($y*10^2$)).

XRPD patterns of electrochemically prepared samples are similar to those of $LiMn_2O_4$. This observation indicates, roughly speaking, a low electron density in the 8*a* tetrahedral site of the spinel structure, and transition metal M (M = Cr, Mn) mainly located in the 16*d* octahedral site. Even after at least 15 cycles, the linewidths remain small, i.e., almost identical to those in the starting compounds (see Fig. 4). (A few tests have shown a slight linewidth increase after 300 cycles). On the other hand, much larger linewidths are observed upon deintercalation (C4.3 and C5.1 compounds). This increase of linewidths and its 2θ dependence strongly suggest a lack of homogeneity, confirmed, as illustrated by Fig. 4, by a significant decrease after relaxation for a long time. It can be noticed that SEM studies performed on samples subjected to several tens of cycles did not reveal any change of the crystals, either in size or in shape.

Preliminary Rietveld refinements were performed considering occupations of 8*a*, 16*d*, and 32*e* sites of space group $Fd\bar{3}m$, and refining the following atomic parameters:

(i) the positional parameter x_O for the oxygen atom in 32*e*,

(ii) an overall thermal parameter U according to the linear constraint: $U_{Li} = U_{Cr} = U_{Mn} = U_O - 0.002$ Å^2. This constraint was retained after many tests to ensure reasonable refinements of site occupancies,

(iii) an occupancy parameter t according to the structural formula:

$$(Li_{x-t}Cr_t)_{Td}[Cr_{y-t}Li_tMn_{2-y}]_{Oh}O_4, \qquad [1]$$

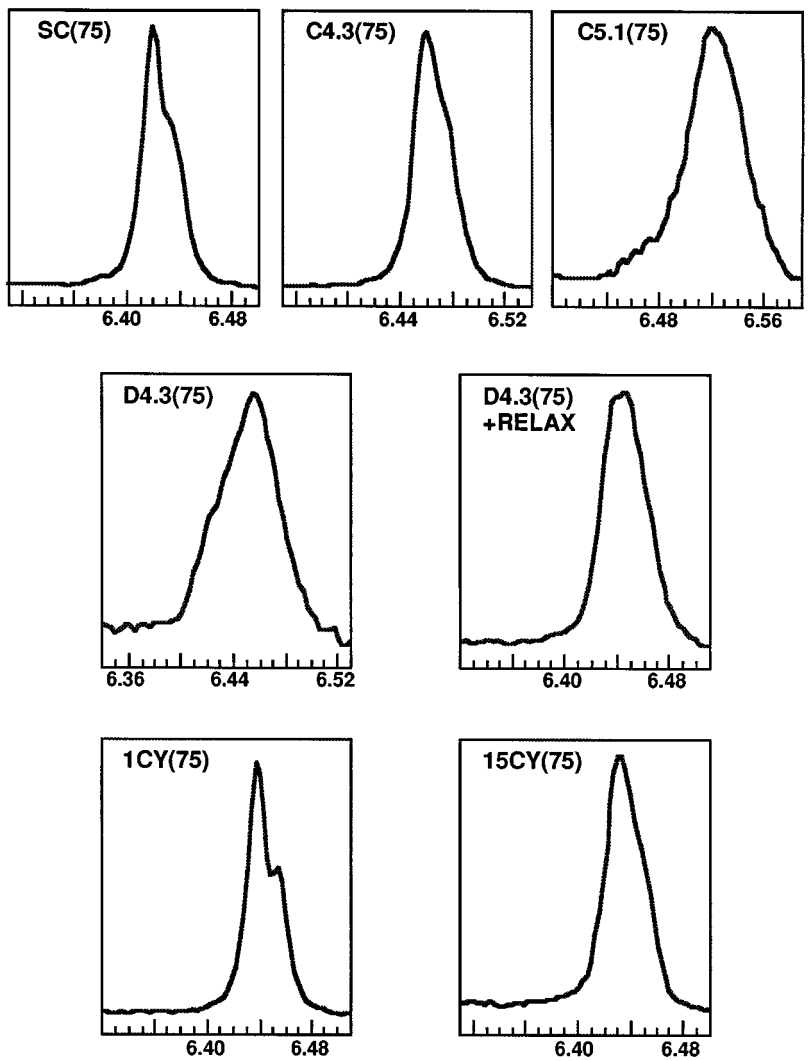

FIG. 4. Profile of the (440) line in the XRPD pattern of the compound with $y = 0.75$ at various steps of the electrochemical treatment.

where Td and Oh stand for 8*a* and 16*d* sites, respectively. It must be mentioned that as Cr and Mn scattering factors are very close to each other it is not possible to distinguish between these two elements in the refinements and formula [1] could be written with some Mn in Td site as well. In the $Li_xCr_yMn_{2-y}O_4$ ($x < 1$) compounds, the Li content x was inferred from the electrochemical curves and therefore the error on x is difficult to estimate; it could be as large as 0.1 and even more after many cycles.

When $x < 1$, the presence of transition metal cations in Td site (hereafter called "Td defect") is not necessarily compensated by the equivalent amount of Li in 16*d* site. However, the Li scattering factor is small compared to those of Mn and Cr and the results of refinements accounting for this possibility (Formula [2]) were not significantly different from those made with the use of Formula [1]. Consequently, meaningful conclusions cannot be drawn from the refinement of Li occupancies.

$$(Li_xM_t\square_{1-x-t})_{8a}[\square_tM_{2-t}]_{16d}O_4, \quad (M = Cr_{y/2}Mn_{1-y/2}). \qquad [2]$$

The refinement conditions indicated above gave satisfactory results in most cases. For a few samples, however, they led to some remaining problems of line intensity. The possibility of M vacancies in 16*d* sites and/or of M occupying other sites was therefore introduced. Among the other "possible" sites for M, i.e., 8*b* and 48*f* (tetrahedral), and 16*c* (octahedral), the 16*c* site was found to be occupied ("16*c* defects"), which implies an equivalent amount of cation vacancies in the 16*d* site. However, in a first approach the two quantities —occupancy of the 16*c* site and amount of vacancies—were refined independently and, as expected, found to be close to each other. Finally, all refinements were made with the use of

$$(Li_{x-\varepsilon}M_t\square_{1+\varepsilon-x-t})_{8a}[Li_\varepsilon M_{2-t-z}\square_{t+z-\varepsilon}]_{16d}(M_z)_{16c}O_4, \qquad [3]$$

with $0 \le x \le 1$; $0 \le \varepsilon \le x$; $0 \le t \le 1-(x-\varepsilon)$; $0 \le z \le 2-t$ and where M is Cr and/or Mn (for each composition the overall M content is $Cr_{y/2}Mn_{1-y/2}$).

Note that M was arbitrarily introduced as Mn in 16*c*, Cr in 8*a*, and that ε was taken as equal to 0. With these refinement conditions, satisfactory results were obtained in all cases.

After the final refinements, all the difference profiles are satisfactory. For the C4.3 and C5.1 compounds however, noticeable remaining peaks due to markedly asymmetric line profiles are observed. Figure 5 shows representative examples of the Rietveld results. All the values of R_{wp} are close to (or even below) R_{Exp}, the highest value corresponding to $\chi^2 = (R_{wp}/R_{Exp})^2 = 3.4$, for SC(25). The reliability factors R_F and R_{F^2} range from 3.7 to 8.2% (for 1CY(25)), with a mean value of 5.4%, and from 3.4 to 10.4% (for 15CY(0)), with a mean value of 5.2%, respectively, for 30 to 33 independent reflections.

Table 2 presents the main structural results (the lattice parameter a, the oxygen coordinate x_O, t, and z) and includes the lithium contents x inferred from the electrochemical experiments. The distances from an 8*a* site and a 16*d* site, to the surrounding oxygen atoms (D_{Td} and D_{Oh}, respectively), calculated from a and x_O, were added in Table 2 since they will appear as meaningful parameters in the following discussion. For D_{Oh}, the "theoretical" value given in parentheses is the distance calculated from the mean ionic radii (7) for the following ions in 16*d*:

(i) $Cr_y^{III}Mn_{1-y}^{III}Mn^{IV}$ in the starting compounds or after n cycles,

(ii) $Cr_y^{III}Mn_{x-y}^{III}Mn_{2-y}^{IV}$ with x close to y in C4.3 and D4.3 compounds,

(iii) $Cr_x^{III}Cr_{y-x}^{IV}Mn_{2-y}^{IV}$ in C5.1 compounds.

In addition to Table 2 the evolution of the above parameters with both the Cr content and the electrochemical treatment is illustrated through Figs. 6 to 10.

Considering first the concentration z of "16*c* defects" it appears (Table 2) that all values are close to zero except for the largest Cr content $y = 0.75$. In that case, Fig. 6 shows that the occupancy of the 16*c* sites becomes significant at the end of the first charge up to 5.1 V. Upon the following discharge down to 4.3 V, a hysteresis phenomenon is observed together with a weak relaxation. At the completion of the first cycle ($n = 1$), the z value is close to zero. For $n = 15$, however, z is no longer negligible and strongly suggests a progressive accumulation of 16*c* defects upon cycling.

The "Td defects" concentrations t are virtually zero in the starting compounds but they become significant after any electrochemical treatment and all the more as the Cr content y increases (Fig. 7). Furthermore, it appears that:

(i) Td defects still exist after a discharge down to 4.3 V, and at the completion of the first cycle

(ii) a long relaxation time slightly lowers t, and

(iii) a progressive accumulation of Td defects (similar to that of 16*c* defects) occurs upon cycling.

Similarly, the D_{Td} and D_{Oh} distances strongly depend both on the electrochemical treatment and the chromium content, as illustrated by Figs. 8 and 9 for $y = 0.25$ and 0.75. Once again changes are more pronounced for the highest chromium concentration. A lowering of D_{Td} occurs upon deintercalation of Li for all compounds (Table 2). For $y = 0.75$ the size of the Td site is significantly reduced after 15 cycles.

In Fig. 9, the D_{Oh} distances, for $y = 0.25$ and 0.75, can be compared to the theoretical values calculated as mentioned above. For $y = 0.25$, experimental and theoretical values are almost identical, except at 5.1 V where the

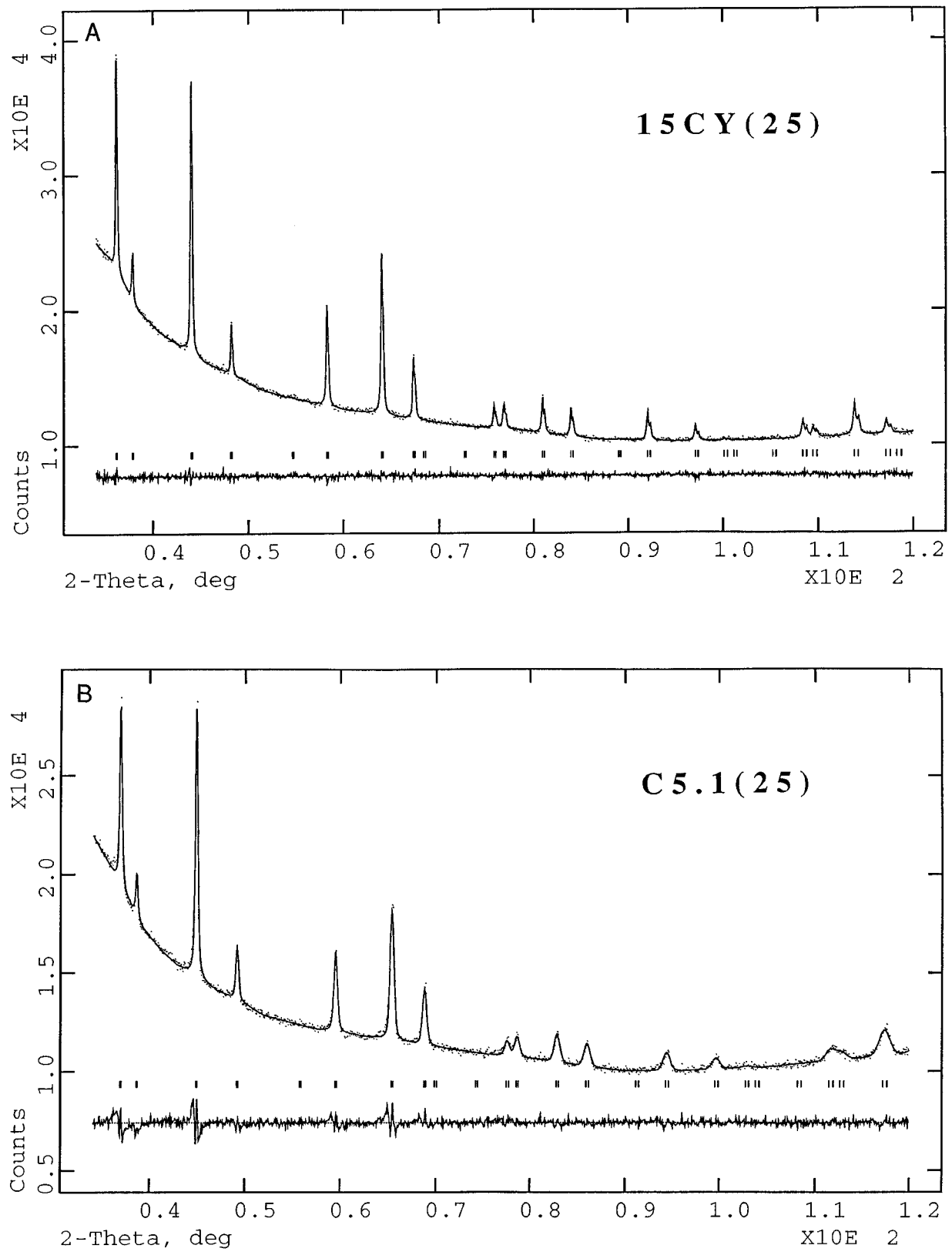

FIG. 5. Representative examples of profiles after Rietveld refinement: experimental (⋯), calculated (—), and difference at the same scale, for: C5.1(25) and 15CY(25).

TABLE 2
Structural Parameters and Cation–Oxygen Distances *D*

Sample and Li content x[a]	Unit-cell parameter a (Å)	Positional parameter x_O	t	z	D_{Td} (Å)	D_{Oh} (Å)
SC(0)	8.2399(1)	0.2627(1)	0.001(3)	− 0.006(2)	1.965(2)	1.961(1)
1.00						(1.967)
C5.1(0)	8.0575(3)	0.2620(2)	0.035(3)	− 0.006(2)	1.912(3)	1.922(2)
0.04						(1.918)
15CY(0)	8.2370(3)	0.2612(3)	0.039(3)	− 0.009(4)	1.943(3)	1.971(2)
1.00						(1.967)
SC(25)	8.2253(1)	0.2619(1)	0.005(2)	− 0.002(2)	1.950(2)	1.964(1)
1.00						(1.964)
C.4.3(25)	8.1342(5)	0.2632(2)	0.022(3)	− 0.004(4)	1.947(3)	1.932(2)
0.36						(1.929)
C5.1(25)	8.0721(4)	0.2620(3)	0.036(4)	0.006(4)	1.916(4)	1.926(2)
0.10						(1.916)
D4.3(25)[b]	8.1214(3)	0.2624(2)	0.020(2)	− 0.002(2)	1.933(3)	1.935(1)
0.36						(1.929)
1CY(25)	8.2249(2)	0.2612(3)	0.021(4)	− 0.007(4)	1.940(4)	1.969(2)
1.00						(1.964)
15CY(25)	8.2256(1)	0.2618(2)	0.026(2)	− 0.004(2)	1.949(2)	1.964(1)
1.00						(1.964)
SC(50)	8.2083(1)	0.2621(1)	0.008(2)	0.002(2)	1.949(2)	1.957(1)
1.00						(1.960)
C.4.3(50)	8.1629(3)	0.2629(2)	0.012(3)	0.000(2)	1.950(3)	1.941(2)
0.57						(1.935)
C5.1(50)	8.0953(5)	0.2616(3)	0.046(4)	0.012(4)	1.915(4)	1.935(2)
0.13						(1.919)
300CY(50)[b]	8.1267(2)	0.2614(2)	0.037(3)	0.000(2)	1.942(3)	1.965(2)
1.00						(1.960)
SC(75)	8.1960(1)	0.2621(1)	0.005(2)	0.000(2)	1.946(2)	1.955(1)
1.00						(1.956)
C.4.3(75)	8.1946(1)	0.2624(1)	0.018(1)	− 0.002(2)	1.951(1)	1.952(1)
0.80						(1.945)
C5.1(75)	8.1169(3)	0.2588(2)	0.103(3)	0.058(2)	1.881(3)	1.960(2)
0.20						(1.924)
D4.3(75)	8.1750(2)	0.2606(2)	0.066(2)	0.030(2)	1.920(2)	1.961(1)
0.80						(1.945)
D4.3(75)[b]	8.1715(4)	0.2607(2)	0.042(3)	0.026(2)	1.920(3)	1.959(2)
0.80						(1.945)
1CY(75)	8.2049(2)	0.2614(1)	0.057(2)	0.004(2)	1.939(2)	1.962(1)
1.00						(1.956)
15CY(75)	8.1891(2)	0.2583(2)	0.091(2)	0.112(2)	1.890(3)	1.982(2)
1.00						(1.956)

[a] Value inferred from the electrochemical curves, for the C and D samples.
[b] Sample allowed to relax for 3 months before the structural study.

decrease of D_{Oh} is slightly less than expected. Differences are much more pronounced for $y = 0.75$; for instance, the deintercalation process up to 5.1 V does not induce any decrease of D_{Oh}.

In the starting compounds, the cell parameter a linearly decreases (from 8.2399(1) to 8.1960(1) Å) when y increases from 0 to 0.75, whereas the C5.1 products show the opposite dependence of a on y (Fig. 10). This means that the amplitude of a variations between SC and C5.1 compounds decreases when the Cr content increases.

The evolution of a in the course of the first cycle and the a values after 15 cycles, for $y = 0.25$ and 0.75, are displayed in Fig. 10 which shows that:

(i) the difference between a values of C4.3 and D4.3 compounds is larger for $y = 0.75$ than for $y = 0.25$,

(ii) the differences between a values of SC, 1CY, and 15CY compounds are negligible for $y = 0.25$ but rather important for $y = 0.75$.

These observations suggest that the structural modifications, which occur upon cycling, increase with the Cr content.

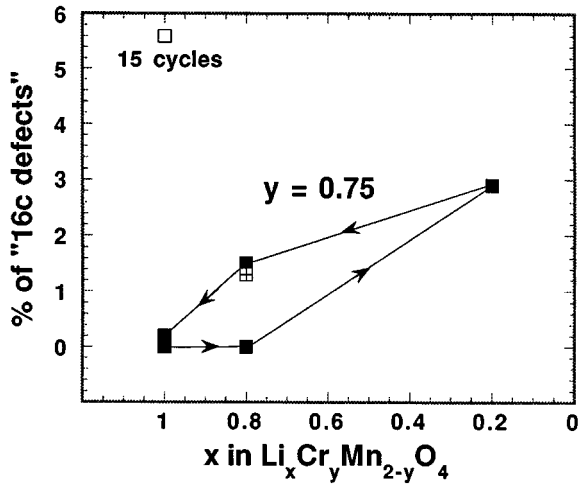

FIG. 6. Percentage of 16*c* defects (i.e., $100 \times z/2$) vs x in $Li_xCr_{0.75}Mn_{1.25}O_4$ at the first cycle and after 15 cycles. The cross represents D4.3(75) allowed to relax for 3 months. The maximum error at 2σ is less than 0.5%.

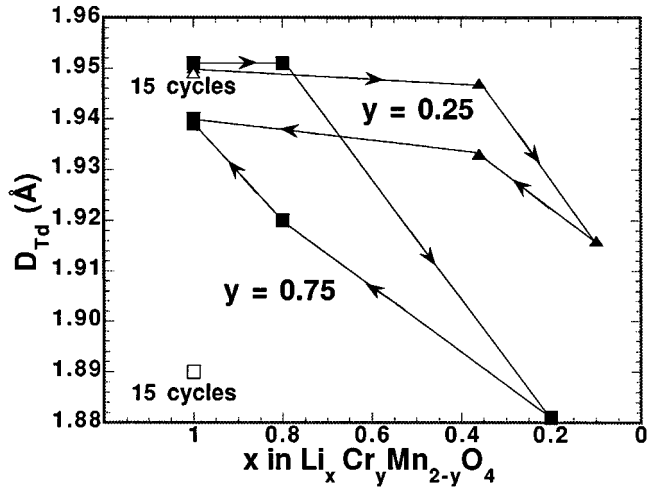

FIG. 8. D_{Td} distances at the first cycle (filled symbols) and after 15 cycles (open symbols). The triangles and squares represent $y = 0.25$ and 0.75, respectively. The mean error at 2σ is less than 0.01 Å.

DISCUSSION

Upon deintercalation up to 5.1 V, the formation of a Td defect, corresponding to a displacement of M cations from a 16*d* to an 8*a* site, induces a significant decrease of D_{Td}, while D_{Oh} do not show the expected decrease, especially for $y = 0.75$. These features strongly suggest a local oxidation of M in tetrahedral site, up to a high oxidation state (such as Cr^{VI}, Mn^{VI}, or Mn^{VII}) leading to a short M–O bond length. This local oxidation would be favored by the 16*d* to 8*a* displacement and stable in this case only. When a Td defect forms, either a vacancy appears in 16*d* or a tetrahedral Li moves to this site; in both cases, it induces an increase of D_{Oh}.

In agreement with the EELS results obtained for the compounds with a high Cr content, it is very likely that some Cr^{VI} cations occupy Td sites at high voltage and, the higher y, the higher the number of $Cr^{VI}O_4$ groups formed and accumulated upon cycling.

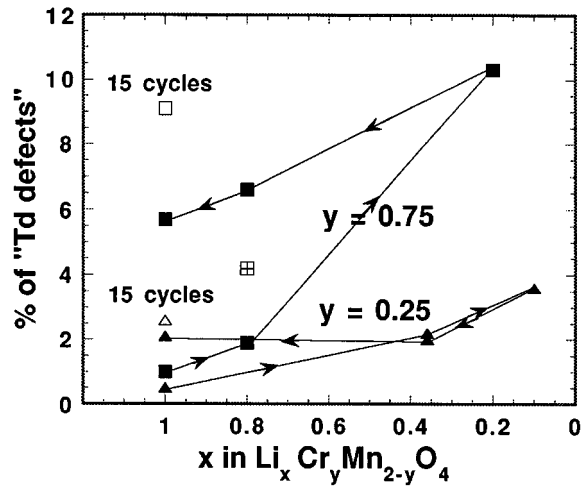

FIG. 7. Percentage of Td defects (i.e., $100 \times t$) vs x in $Li_xCr_{0.25}Mn_{1.75}O_4$ and $Li_xCr_{0.75}Mn_{1.25}O_4$, during the first cycle (filled symbols) and after 15 cycles (open symbols). The cross represents D4.3(75) allowed to relax for 3 months. The triangles and squares represent $y = 0.25$ and 0.75, respectively. The mean error at 2σ is 0.7%.

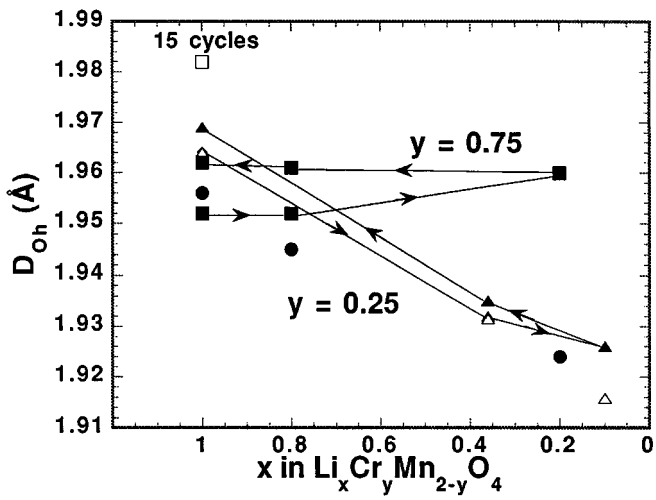

FIG. 9. D_{Oh} distances. The triangles and squares (filled symbols) represent $y = 0.25$ and 0.75, respectively, at the first cycle. The open triangles and filled circles represent "theoretical" distances (see text) for $y = 0.25$ and 0.75, respectively. The open square represents $y = 0.75$ after 15 cycles. The mean error at 2σ is less than 0.005 Å.

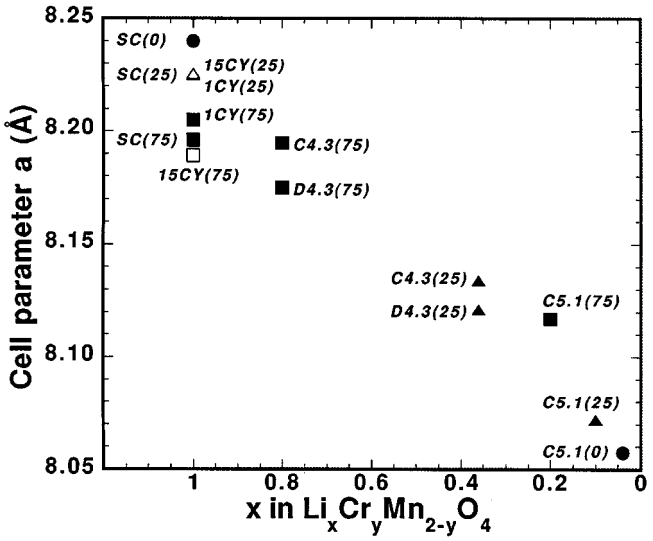

FIG. 10. Evolution of the cell parameter a (Å) vs x, and depending on the electrochemical treatment, for various Cr contents. The maximum error at 2σ is 1.5×10^{-3} Å.

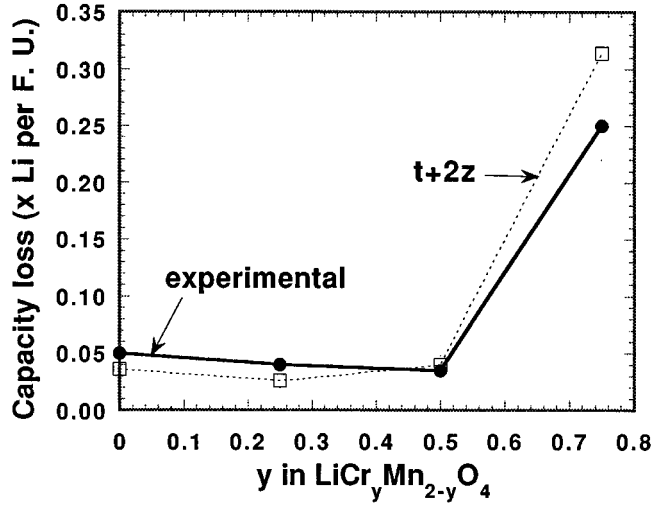

FIG. 11. Evolution of the experimental capacity loss (filled circles) and of the loss $(t + 2z)$ expected from structural study (squares), after 15 cycles, as a function of the Cr content. The experimental loss is the difference between the number of Li intercalated during the 1st and 16th discharges.

Upon intercalation, most of the Td defects disappear due to reduction. Nevertheless, an accumulation of Td defects is detected in all *n*CY compounds, which raises the question, remaining unanswered, of the presence of tetrahedral Cr (or Mn) cations (likely with a high oxidation state) after the discharge.

At 5.1 V, as most of the Td sites are empty, the formation of 16*c* defects corresponds to local modifications toward a rock salt structure. Note that the 16*c* site is larger than the 16*d* (2.12 Å instead of 1.95 Å, approximately), so that it should better accomodate a M^{III} cation than a M^{IV}. Nevertheless, the formation of a 16*c* defect upon oxidation and that could contain a M^{III} cation is puzzling. However, considering for instance the C5.1(75) compound with $t = 0.10$, the tetrahedral M cations (Td defects) are supposed to be highly charged and, according to the EELS results, likely to be Cr^{VI}. If so, each Td defect implies two additional charges with respect to a "normal" octahedral Cr^{IV}, and these charges must be balanced by two octahedral M^{III} cations. Taking into account the composition $Li_{0.20}Cr^{VI}_{0.10}Cr_{0.65}Mn_{1.25}O_4$ in C5.1(75), and the main conclusions of the EELS study, one can estimate the $Mn^{III}:Mn^{IV}$ ratio as 3 : 7. These values agree with the profile of the EELS spectrum and with the features already discussed for D_{Oh}. An explanation of this puzzling situation could be provided by a local crystal field stabilization of Mn^{III}, which is quite possible in such a disordered structure. Part of the Mn^{III} cations could be stabilized in 16*c* sites, which are larger than 16*d*.

What is the influence of Td and 16*c* defects on the number of Li that can be reversibly intercalated in the structure and especially of 8*a* Li ions, since their number probably determines the maximum capacity of the batteries in the range 3.5–5.1 V? It is obvious that a Td defect eliminates a tetrahedral Li site. An octahedral 16*c* site shares two faces with tetrahedral 8*a* sites and the 16*c*–8*a* distance is short: ~ 1.8 Å. Therefore, the formation of 16*c* defects implies (at least) twice as many Td vacancies, i.e., twice as many tetrahedral sites no longer accessible to Li ions. If one now considers the 15CY(75) compound, which exhibits many defects ($t = 0.09$; $z = 0.11$), the formula

$$(Li_{0.69-\beta}Cr_{0.09}\square_{0.22+\beta})_{8a}[Li_{\alpha}Cr_{0.66}\square_{0.2-\alpha}Mn_{1.14}]_{16d}$$
$$(Mn_{0.11})_{16c}O_4, \quad 0 \le \beta \le 0.69 \quad 0 \le \alpha \le 0.2, \qquad [4]$$

illustrates the limits implied by the defects (M is introduced arbitrarily as Cr in 8*a* and Mn in 16*c*). As already mentioned, the structural study could not provide precise informations on α and β. Nonzero α corresponds to additional defects. The β value is expected to be zero (it is close to zero, considering the experimental capacity of the corresponding battery). Nevertheless a nonzero β could arise from numerous possible limitations of the reversibility. Anyway, the maximum number of tetrahedral Li is $1 - (t + 2z)$, that is 0.69 in Formula [4]. Consequently, after n complete cycles, the capacity should drop at least down to $100[1 - (t + 2z)]$ percent of the initial capacity. The experimental capacity loss after 15 cycles (*3*) (loss expressed as a number of Li per $Li_xM_2O_4$ formula) can be compared, in Fig. 11, to $(t + 2z)$ for some 15CY compounds. The observation of the good correlation indicates that the structural defects are likely the main cause of the progressive capacity fading, at least for $y = 0.75$.

The detrimental effect of Cr on the capacity retention, at high Cr content, has supplementary explanations. On the one hand, a 16*c* defect should lower the mobility of Li, since the 16*c* site is situated on the diffusion path of Li. On the other hand, the higher the defect concentration, the smaller the Td sites, which therefore become still more convenient for highly charged cations. At high Cr content, the formation of tetrahedral Cr^{VI}, which is likely, well explains the rapid capacity loss by a high defect rate favoring accumulation of supplementary defects.

Conversely, at low Cr content, i.e., $y \approx 0.25$, the capacity retention is improved with respect to $LiMn_2O_4$. As the defect rates remain low and similar for $y \leq 0.5$, the defects could play an indirect role in this improvement. Indeed, the beneficial role of Cr could be due to the dependence of the cell parameter *a* on *y*: the smaller the lowering of *a* during the charge, the better the Li diffusion and the reversibility of defects formation via displacements of *M*; a lowering of elastic strains in the crystals can also play a beneficial role.

CONCLUSION

The electrochemical Li deintercalation from the compounds $LiCr_y^{III}Mn_{1-y}^{III}Mn^{IV}O_4$, $0 \leq y \leq 1$, induces a migration of some transition metal cations from 16*d* to 8*a* sites of the spinel structure. This formation of so called Td defects upon oxidation is not completely reversible; therefore an accumulation of Td defects is observed upon cycling that becomes all the more important as the Cr content increases. Simultaneously, but only at high Cr content ($y > 0.50$), some transition metal cations move to 16*c* sites and an accumulation of such 16*c* defects is also observed.

On account of EELS results and in agreement with structural features, Td defects would correspond to Cr^{VI} cations mainly, whereas 16*c* defects could result from a local crystal field stabilization of Mn^{III} cations.

Both types of defects render some Td sites no longer accessible to Li ions and this feature well explains the capacity loss observed upon cycling.

REFERENCES

1. J.-M. Tarascon, E. Wang, F. K. Shokoohi, W. R. McKinnon, and S. Colson, *J. Electrochem. Soc.* **138,** 2859 (1991).
2. T. Yoshinori and M. Yasuhiko, "Kokkai Tokkyo Koho," JP 04,141,954 [92,141,954], May 15, 1992.
3. C. Sigala, D. Guyomard, A. Verbaere, Y. Piffard, and M. Tournoux, *Solid State Ionics* **81,** 167 (1995).
4. R. J. Hill and I. C. Madsen, *Powder Diffraction* **2**(3), 146 (1987).
5. A. C. Larson and R. B. Von Dreele, "Generalized Structure Analysis System," Los Alamos, University of California, 1994.
6. J.-L. Mansot, P. Leone, P. Euzen, and P. Palvadeau, *Microsc. Microanal. Microstruct.* **5,** 79 (1994).
7. R. D. Shannon, *Acta Crystallogr. A* **32,** 751 (1976).